High-pressure stability of Cs_6C_{60}

R. Poloni,[1,2,*] D. Machon,[1] M. V. Fernandez-Serra,[3] S. Le Floch,[1] S. Pascarelli,[2] G. Montagnac,[4] H. Cardon,[4] and A. San-Miguel[1]

[1]*Laboratoire PMCN, CNRS, UMR 5586, Université Lyon 1, Université de Lyon, F-69622 Villeurbanne Cedex, France*

[2]*European Synchrotron Radiation Facility, B.P. 220, F-38043 Grenoble, France*

[3]*CECAM, ENS-Lyon, 46 Allée d'Italie, F-69007 Lyon, France*

[4]*Laboratoire de Sciences dela Terre, ENS-Lyon, Université Lyon 1, Université de Lyon, F-69364 Lyon, France*

(Received 7 September 2007; revised manuscript received 12 February 2008; published 14 March 2008)

The Cs_6C_{60} molecular crystal has been studied by Raman spectroscopy measurements and *ab initio* calculations under high pressure. The Raman scattering data have been collected from ambient pressure up to 45.5 GPa at room temperature. It is shown that the intercalation of cesium atoms in the C_{60} crystalline structure allows us to preserve the C_{60} molecules up to the maximum studied pressure, i.e., more than twice the amorphization pressure of the solid C_{60} fullerene crystal. The calculated pressure evolution of all the observed Raman mode frequencies is in good agreement with that obtained experimentally. In this work, the high-resolution measurements allow us to observe six Raman modes and several partners in doublets in addition to the Raman lines previously observed for the same system. The symmetry of all the observed modes has been identified through our calculations.

DOI: 10.1103/PhysRevB.77.125413 PACS number(s): 78.30.Na, 62.50.−p, 31.15.A−

The C_{60} fullerene and its compounds have attracted much attention due to some of their extraordinary properties, related to the high symmetry and simplicity of the molecule. Among these, the compressibility of the single buckminsterfullerene molecule has been calculated to have values between 700 and 900 GPa,[1,2] highly exceeding that of diamond (around 440 GPa). This makes the C_{60} molecule a good candidate for the constitution of a molecular solid able to sustain very high pressures, a domain that is usually reserved to simple molecular systems, with a very limited number of atoms as diatomic molecular solids. In the pristine fcc structure, i.e., the natural association of the C_{60} fullerenes, such expectations are frustrated by the interaction between molecules, which leads to the amorphization of the structure observed at 22 GPa at room temperature.[3,4] From that pressure, the signature of the molecule integrity, corresponding to the Raman molecular modes, is lost, implying the destruction of the molecule. At high temperature, the stability of the molecular C_{60} solid is limited by the formation of covalent intermolecular bondings, giving rise to one-dimensional, two-dimensional (2D) or 3D polymers starting at pressures lower than 1 GPa.[5–13] In such a case, the cagelike structure can be preserved, leading, nevertheless, to the loss of the molecular character of the crystal.

In the present work, we show that the intercalation of solid C_{60} with Cs alkali atoms, leading to the formation of the Cs_6C_{60} compound, allows us to bypass such limitation, warranting the stability of the C_{60} molecules at pressures of at least 45 GPa.

The sample consisting of the Cs_6C_{60} powder compound was prepared by mixing stoichiometric amounts of C_{60} and Cs in inert atmosphere, as described in Ref. 14. The characterization of the sample was performed by x-ray diffraction, and the obtained structural parameters are in good agreement with those reported in literature.[15,16] The sample was loaded into a gasketed diamond anvil cell in a glove box using solid NaCl as a pressure transmitting medium. The pressure was calibrated by the R1 fluorescence line of a ruby chip placed in the vicinity of the sample. Ambient pressure Raman scattering data were collected on a sample powder loaded into a capillary in inert atmosphere.

High-resolution ($\sim$0.5 cm^{-1}) Raman measurements were recorded on a Jobin-Yvon HR-800 Labram spectrometer with double-notch filtering and air cooled charge coupled device detector used in backscattering geometry. The laser beam (514.5 nm exciting lines of an Ar^+ laser) was focused down to a 2 μm spot on a sample.

For the isolated C_{60} molecule with I_h symmetry, only 10 of the 46 calculated vibrational modes are Raman active ($2A_g+8H_g$). For the solid fcc C_{60} system, the symmetry-lowering perturbation due to the crystal field associated with the condensed phase gives rise to a very large number of allowed Raman modes. A group theoretical analysis performed by Dresselhaus *et al.*[17] showed that the solid C_{60} with a T_h^6 symmetry displays 29 one-dimensional A_g modes, 29 two dimensional E_g modes, and 87 three-dimensional T_g modes. Nevertheless, several experiments[4,18,19] suggested that most of these modes are very weak or give rise to small unresolved splittings of the ten main Raman-allowed modes of the isolated molecule.

For the fully doped Cs_6C_{60} compound with a T_h^5 symmetry, calculations[17] show that each of the five-dimensional H_g modes appearing in the isolated C_{60} molecule splits into two-dimensional E_g and three-dimensional T_g modes. Moreover, the $3T_{1g}$, $4T_{2g}$, and $6G_g$ modes in the I_h symmetry should become weakly Raman active, changing their symmetry into $3T_g$, $4T_g$, and $6(A_g+T_g)$, respectively.

Low-resolution (6 cm^{-1}) Raman measurements performed at ambient conditions for the fully doped systems M_6C_{60} (with M=K, Rb, and Cs) have been previously reported.[16,17,19] In that work, ten Raman modes corresponding to the Raman active modes of the isolated molecule were observed. Hence, they labeled for commodity these vibrations with the names of the irreducible representation of the Raman active modes of the isolated C_{60} molecules with I_h

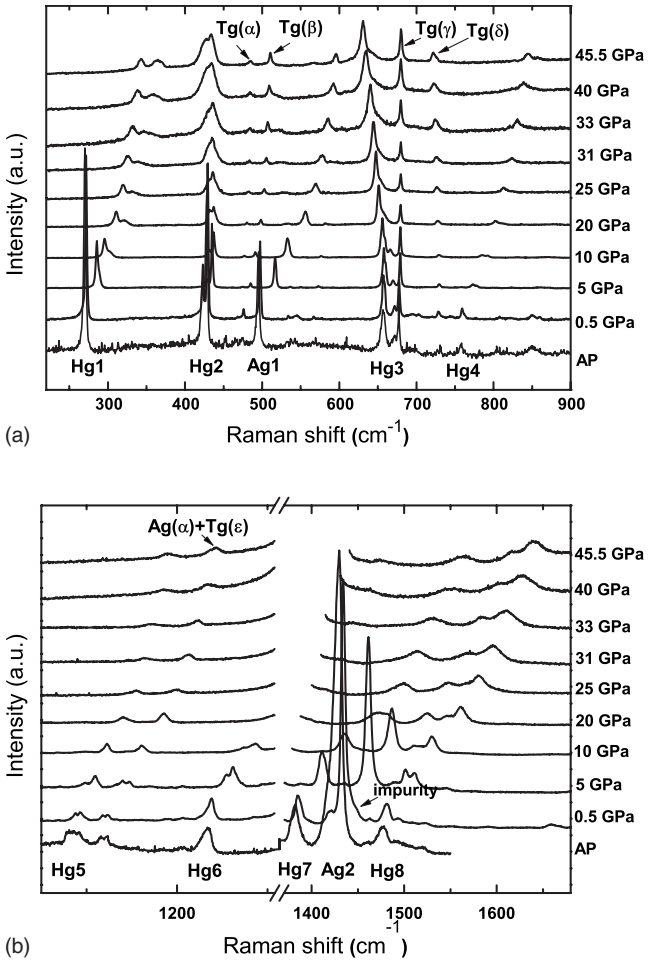

FIG. 1. Low-frequency (left panel) and high-frequency (right panel) Raman spectra of Cs_6C_{60} at room temperature as a function of pressure. The modes are labeled with the names of the irriducible representation of the Raman active modes of the free C_{60} molecule for commodity. A continuous evolution of the intramolecular Raman modes under pressure is observed up to 45.5 GPa. The Raman mode intensity has been normalized to the $H_g(3)$ (first line) intensity mode in the upper panel and to the $H_g(7)$ intensity mode in the lower panel. The Raman spectrum at 0.5 GPa shows the presence of a shoulder in the $A_g(2)$ mode coming from an impurity also found on the gasket.

symmetry, i.e., $2A_g+8H_g$. In addition, the authors also observed five new lines, corresponding to partners in doublets. In particular, for the Cs_6C_{60} system, four of the H_g modes $[H_g(2), H_g(3), H_g(5)$, and $H_g(7)]$ were split into doublets of a measurable amount. For K_6C_{60} and Rb_6C_{60}, they also observed a splitting of the $H_g(1)$ mode into a doublet. A more detailed discussion about theoretical prediction compared to experimental observation of lines in M_6C_{60} solids due to the symmetry lowering from I_h to T_h^5 can be found in Ref. 17.

In the present work, we observe six Raman modes and eight partners in doublets in addition to the ten Raman active modes of the isolated molecule. The behavior of all the observed lines is followed with pressure.

In Fig. 1, we display the Raman scattering spectra in the frequency regions 220–900 and 1050–1680 cm^{-1}, at various pressures at room temperature. In the following, we refer to the previously ten observed intramolecular Raman vibrations as the $2A_g$ and $8H_g$ symmetry modes of the free molecule in order to keep the same nomenclature used in the past. On the other hand, we label the observed lines according to the symmetry of irreducible representation of the Raman active modes of the Cs_6C_{60} system with a T_h^5 space group.

The Raman spectra of Cs_6C_{60} were measured from ambient pressure up to 45.5 GPa at room temperature. Only part of all collected spectra are represented in Fig. 1 for clarity.

The six modes are labeled in Fig. 1 as $T_g(\alpha)$, $T_g(\beta)$, $T_g(\gamma)$, $T_g(\delta)$, $T_g(\epsilon)$, and $A_g(\alpha)$, and their symmetry has been identified through our *ab initio* calculations. Many other low-frequency Raman active modes of solid Cs_6C_{60} associated with intermolecular and molecule–alkali metal motions have been anticipated, but they have not yet been observed as they are too weak to be experimentally detected.

Let us first discuss our Raman spectrum at ambient pressure. The ambient pressure frequency of all the observed Raman modes is reported in Table I. The ambient pressure data have been collected on a sample in a closed glass capillary, and they show lower quality compared to the high-pressure spectra. It is then less evident to distinguish the $T_g(\alpha)$ and $T_g(\beta)$ modes whose evolution as a function of pressure has been clearly followed. For these two modes, the ambient pressure Raman frequency has been extrapolated by using the pressure evolution fitted curves.

The Raman shifts measured for the previously observed Cs_6C_{60} modes are in good agreement with those reported in the published works.[16,17,19]

In Table I, we list the symmetry of the experimentally observed Raman modes in the alkali-metal-doped C_{60} system and the corresponding mode symmetry of the isolated fullerene.

In the following, the Cs_6C_{60} Raman spectra evolution under pressure is discussed. In Fig. 1, we show the evolution of the Raman spectra as a function of pressure from ambient pressure up to 45.5 GPa, and in Fig. 2 the pressure evolution of the Raman frequencies. The continuous evolution of all the Cs_6C_{60} Raman modes as a function of pressure up to 45.5 GPa proves that the presence of a heavy alkali metal in solid C_{60} contributes to an increase in the pressure stability region of the C_{60} molecules of more than 100% in comparison to pristine fcc C_{60} where previous studies have shown an irreversible transition at 22 GPa accompanied by the loss of the intramolecular C_{60} modes.[4,20] In Fig. 1, we observe that most lines show a pressure increase of their frequency with the exception of $H_g(2)$, $H_g(3)$, and $T_g(\delta)$, which slightly soften linearly with pressure and the $T_g(\alpha)$ and $T_g(\gamma)$ modes, which essentially do not show any change in frequency. A Raman spectrum collected at a pressure of 5 GPa after pressure release from the highest measured pressure shows that the Raman mode evolution is reversible.

The evolution of the Raman spectra with pressure has been firstly considered in a reduced range of pressure (up to 22.3 GPa) in order to compare our results with those previously obtained for the nonintercalated solid C_{60} (see Table I) up to 22 GPa. In this limited range of pressure, the frequency evolution of the observed Raman modes can be considered a linear function of pressure, with good approximation. The

TABLE I. Symmetry of the observed Raman modes in the Cs_6C_{60} system and the corresponding Raman mode symmetry in the isolated molecule. The experimentally measured ambient pressure frenquecies are compared to the theoretical values. The left side of the table reports the first and second derivatives of the least-square fit curves of the parabolic pressure dependence of all modes for both experiments and calculations. In the latter case, a fit up to 43 GPa, instead of 98 GPa, has been considered to better compare the results with the experiment. The right side of the table lists the first derivative of the least-square fit curves of the linear pressure dependence (considered up to 22.3 GPa) of all Cs_6C_{60} modes. The values previously obtained for the solid C_{60} are also reported for comparison. The "*" symbols refer to the T_g symmetry modes. The "†" symbol indicates that the fit was not possible due to the scarcity of lines observed under pressure.

Mode C_{60} I_h	Mode Cs_6C_{60} T_h^5	ω_0 (cm^{-1}) Cs_6C_{60} Expt.	ω_0 (cm^{-1}) Cs_6C_{60} Calc.	$\partial\omega/\partial P$, $\partial^2\omega/\partial P^2$ (cm^{-1}/GPa, cm^{-2}/GPa^2) Cs_6C_{60} up to 45.5 GPa Expt.	$\partial\omega/\partial P$, $\partial^2\omega/\partial P^2$ (cm^{-1}/GPa, cm^{-2}/GPa^2) Cs_6C_{60} up to 43 GPa Calc.	$\partial\omega/\partial P$ (cm^{-1}/GPa) C_{60} up to 22 GPa Ref. 20, Ref. 4	$\partial\omega/\partial P$ (cm^{-1}/GPa) C_6C_{60} up to 22.3 GPa This work
$H_g(1)$	$E_g(1)+T_g(1)$	269.9	261.5*	2.4/−0.02	3.2/−0.02	1.1	2.0
		†	262.6	2.6/−0.01	3.1/−0.02		2.2
$H_g(2)$	$E_g(2)+T_g(2)$	422.3	406.7*	0.6/−0.01	0.7/−0.01	2.4, 0.16	0.3
		427.6	410.8	0.6/−0.01	0.5/−0.01		0.3
T_{2g}	$T_g(\alpha)$	460.3	450.8	0.7/−0.01	0.8/−0.01		0.5
T_{1g}	$T_g(\beta)$	476.0	452.2	1.4/−0.02	1.7/−0.02		1.1
$A_g(1)$	$A_g(1)$	494.9	496.7	3.8/−0.04	3.7/−0.02	0.75, 0.94	3.0
$H_g(3)$	$E_g(3)+T_g(3)$	657.5	632.4	−0.2/−0.01	−0.2/−0.01	−0.92, −0.55	−0.4
		658.9	633.6*	0.1/−0.01	−0.2/−0.01		−0.2
T_{2g}	$T_g(\gamma)$	677.1	702.4	0.1/−0.001	0.2/−0.01		0.1
$H_g(4)$	$E_g(4)+T_g(4)$	755.9	762.0	2.7/−0.02	3.1/−0.02	−0.71, −0.50	2.3
		759.0	765.0*	3.1/−0.02	4.1/−0.04		2.6
T_{2g}	$T_g(\delta)$	730.6	766.7	−0.02/−0.003	1.0/−0.01		−0.1
$H_g(5)$	$E_g(5)+T_g(5)$	1081.9	1100.6*	2.9/−0.02	3.6/−0.03		2.6
		1090.0	1100.7	3.8/−0.03	4.1/−0.03		2.4
G_g	$A_g(\alpha)+T_g(\epsilon)$	1116.0	1134.3	†	4.7/−0.04		3.4
		1122.1	1139.2*	3.8/−0.03	4.4/−0.03		3.3
$H_g(6)$	$E_g(6)+T_g(6)$	1229.3	1271.7*	5.2/−0.08	6.6/−0.06		4.3
		1235.6	1278.2	5.2/−0.04	6.9/−0.06		4.8
$H_g(7)$	$E_g(7)+T_g(7)$	1382.0	1441.7	4.9/−0.02	6.8/−0.05	4.12, 2.4	4.4
		NO	1450.4*		7.0/−0.06		†
$A_g(2)$	$A_g(2)$	1429.0	1489.0	5.2/−0.03	8.2/−0.07	3.11, 1.7	4.5
$H_g(8)$	$E_g(8)+T_g(8)$	1476.8	1522.1	4.2/−0.05	6.3/−0.05	2.73, 3.7	3.4
		1491.6	1528.9*	3.7/−0.01	5.9/−0.04		3.5

pressure dependence of the eight H_g lines associated with intramolecular vibrations is similar to that of solid fcc C_{60}, while the Raman frequency of the two A_g modes show a stronger dependence on pressure than for pristine C_{60}.[4,20] In fact, the Raman shift of the $A_g(1)$ mode increases as a function of pressure, and its slope (3.0 cm^{-1} GPa^{-1}) is approximatively four times larger than in pristine C_{60} (0.75 cm^{-1} GPa^{-1} in Ref. 20 and 0.94 cm^{-1} GPa^{-1} in Ref. 4). As $A_g(1)$ is a nearly 100% radial mode,[21] in the case of alkali metal intercalated C_{60}, namely, Cs_6C_{60}, the presence of Coulomb interactions contributes to rapidly increasing the "breathing" mode frequency with pressure, more than in the nonintercalated solid C_{60}. The compression of the C_{60} molecules with pressure,[14] coupled to the presence of ionic interactions in the system, is probably responsible for such high value of the pressure derivative of the $A_g(1)$ mode in Cs_6C_{60}. The frequency increase of the $A_g(1)$ radial mode upon doping was previously explained by Jishi and Dresselhaus[22] by considering the variation in the electric field at the sites of the negatively charged carbon during a vibration. This variation produces an extra radial force on these atoms responsible for the increase in the bond-stretching force constant. In addition, the effect of pressure is to decrease the separation between the centers of the ions and the C_{60} sphere, causing an increase in the electrostatic interaction and, finally, an increase in the Raman shift frequency of the $A_g(1)$ vibration. This is very similar to the case of alkali metal intercalated systems with small dopant ions whose increase in the $A_g(1)$ mode frequency with respect to solid C_{60} has been observed to be bigger than for larger alkali metals.[16]

For the pentagonal-pinch $A_g(2)$ mode, we have found a value of 4.5 cm^{-1} GPa^{-1}, which is much larger than the values obtained for solid C_{60}.[4,20] On the other hand, this value is

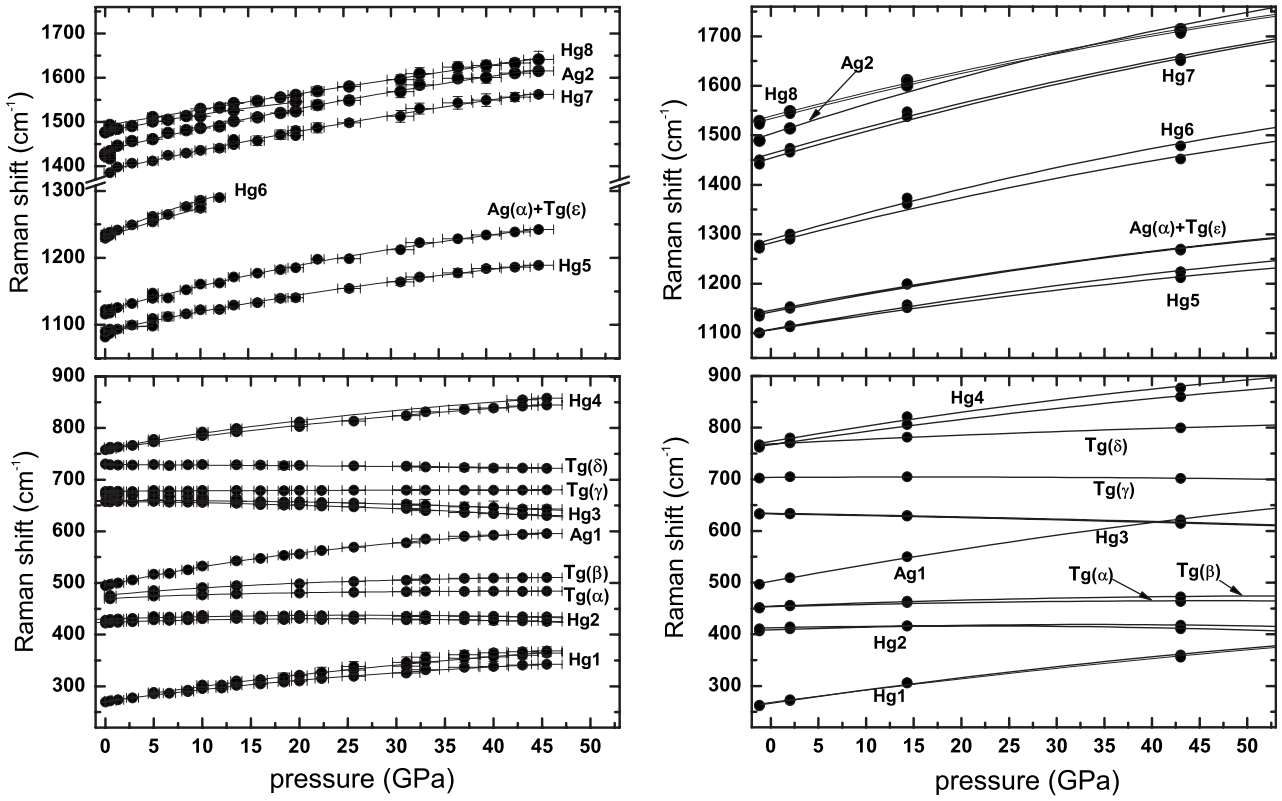

FIG. 2. Pressure dependence of the low-frequency and high-frequency Raman modes of Cs_6C_{60} from ambient pressure up to 45.5 and 43 GPa, as obtained from experiments (left panels) and calculations (right panels), respectively. The solid lines correspond to least-squares fits of a parabolic pressure dependence for most modes. The horizontal error bar represents the pressure uncertainty estimated from the Lorentzian width of the ruby R1 line; the vertical error bar is the half-width at half maximum of each Raman mode.

very close to that found for Cs_3C_{60} by Fujiki *et al.*,[23] which is 4.0 cm^{-1} GPa^{-1}. We want to reiterate here that the $A_g(2)$ mode, which is a nearly 100% tangential mode, has been observed to soften after the intercalation of Cs atoms (6 cm^{-1}/alkali metal) into the C_{60} lattice at ambient pressure[16,19] due to the elongation of the average C-C bond length caused by the charge transfer to the antibonding lowest unoccupied molecular orbital states of the C_{60} molecule.[24] Then, we observe that in Cs_6C_{60} compounds (as also in the case of Cs_3C_{60}), the application of pressure increases the intraball force constant of the C_{60} molecule, more than in the case of pristine C_{60}.

Finally, the two $T_g(3)$ and $E_g(3)$ soft modes [derived from the $H_g(3)$ mode] in Cs_6C_{60} are harder than in the pristine C_{60} system. The most intense line at 657.5 cm^{-1} at ambient pressure has a pressure coefficient of −0.4 cm^{-1} GPa^{-1}, which is 30% and 57% smaller than the values observed for the $H_g(3)$ mode in solid C_{60}.[4,20] This could be considered a signature of the higher stability of the fullerene molecule in Cs_6C_{60} with respect to the nonintercalated C_{60}.

When considering the pressure evolution of the Raman modes up to 45.5 GPa, it turns out that their dependence as a function of pressure is no more linear for the majority of the Raman lines (Fig. 2). A parabolic function, which constitutes a first approximation of an exponential-decay function, is able to reproduce the behavior of the Raman modes with pressure. This can be considered as an indication of anharmonic effects.[25] In Table I, we report the linear and quadratic terms corresponding to the parabolic fit of the pressure dependence of the observed Raman modes up to 45.5 GPa.

Parallel to experiments, we performed density functional *ab initio* simulations to calculate the zone center vibrational modes of Cs_6C_{60} under pressure.

In particular, we have used the SIESTA (Ref. 26) method, where the eigenstates of the Kohn–Sham Hamiltonian are expressed as linear combinations of numerical atomic orbitals. We have used variationally optimized[27,28] double-ζ polarized basis sets. Real space integrals were performed on a mesh with a 310 Ry cutoff. We worked within the local density approximation (LDA) to the exchange and correlation potential.[29]

Core electrons are replaced by nonlocal, norm-conserving fully separable Troullier–Martins pseudopotentials. In the calculations, 2*s* and 2*p* orbitals of C atoms were explicitly included in the valence. For the Cs atoms, we included both semicore and valence orbitals (6*s* and 5*p*) as their inclusion was found to be critical in order to correctly predict the structural properties of this compound.

We studied the Raman mode frequency evolution of Cs_6C_{60} as a function of pressure by decreasing the lattice parameter from the experimental value found at ambient pressure and room temperature (a=11.79 Å) down to 10.00 Å. This corresponds to the pressure range [−1.2,98] GPa. For the different volume values, we have minimized the total energy until the forces on atoms were smaller than 0.04 eV/Å.[14]

The bcc unit cell contains a total of 66 atoms, and sampling of the reciprocal space was performed using a $2\times2\times2$ Monkhorst–Pack mesh. We obtain the dynamical matrix using a finite difference approach, where the atoms were displaced by $\Delta x=0.2$ Å. The Hellmann–Feynman forces were calculated for all the atoms in the system, fully building the dynamical matrix.

We used a bond polarizability model, reported in Ref. 30, to calculate the intensity of the first-order off-resonance Raman scattering. The Raman polarizability parameters of single and double bonds in C_{60} are those reported in the same work and are obtained by fitting experimental off-resonance Raman spectra with such a model. The predicted intensity is somewhat different from that experimentally observed. This is due to the fact that the polarizability parameters for C atoms in Cs_6C_{60} should radically differ from those in the isolated C_{60} because of the charge transfer and also because the single and double bond lengths change with pressure. Indeed, the higher the pressure is the worse the prediction of the Raman intensities is, an indication of the degradation of the original polarizability parameters. However, the model is a practical tool to easily identify the Raman activity of the modes, allowing us to tightly discriminate between all the 192 modes in the spectrum.

We studied the frequency evolution of Raman active modes, as obtained by *ab initio* calculations together with the polarizability model. The results are reported in Fig. 2 and Table I. We report only the theoretical results obtained up to 43 GPa for a clearer comparison with experiments. Nevertheless, the calculations show that all Raman modes observed at low pressures remain active even at very high pressure (98 GPa). The ten Raman modes $(2A_g+8H_g)$ experimentally observed and previously labeled for commodity with the names of the irreducible rapresentation of the Raman active modes of the isolated C_{60} molecule have been well identified in our calculations.

We observed a splitting of each H_g mode into a two-dimensional E_g mode and a three-dimensional T_g mode, as predicted by group theory[17] and as observed from our experiments. Moreover, the six observed lines, labeled as $T_g(\alpha)$, $T_g(\beta)$, $T_g(\gamma)$, $T_g(\delta)$, $T_g(\epsilon)$, and $A_g(\alpha)$, have been well identified in this study, and they have all been found to have a three-dimensional T_g symmetry except for the $A_g(\alpha)$ mode. The calculated first and second derivatives of the pressure dependence of the frequencies of all the Raman modes are reported in Table I for a comparison with the experimental obtained values. The fitted curves of the calculated pressure evolution frequencies reported in Table I have been considered only up to 43 GPa to better compare experiments and theory. A good agreement between experiments and calculations is observed.

Both experiments and calculations allow us to conclude that the molecular character of the C_{60} fullerene can be maintained through alkali intercalation up to pressures at least two times higher (around 45 GPa) than for the previously reported solid C_{60} (around 22 GPa).[31] At the same time, as recently shown in a previous study perfomed up to 15 GPa,[14] a progressive pressure-induced deformation of the molecule takes place due to the pressure enhanced Coulombic interaction between the fullerene and the alkali metal atoms. By calculating the distortion parameter, which has been defined in Ref. 14, we observe that at 43 GPa the deformation of the C_{60} molecule is 32% higher than at about 15 GPa. Our study shows that in spite of such slight deformation, the molecular character of the 60-atom fullerene is maintained. This will allow us to envisage fullerene exohedral intercalation as a path to preserve the properties of encapsulated atoms or molecules in these or larger fullerenes at very high pressures.

*Present address: Institut de Ciència de Materials de Barcelona (CSIC), Campus de la UAB, E-08193 Bellaterra, Barcelona, Spain.

[1] S. J. Woo, S. H. Lee, E. Kim, K. H. Lee, Y. H. Lee, S. Y. Hwang, and I. C. Jeon, Phys. Lett. A **162**, 501 (1992).
[2] R. S. Ruoff, Nature (London) **350**, 663 (1991).
[3] M. Núñez-Regueiro, P. Monceau, and J.-L. Hodeau, Nature (London) **355**, 237 (1992).
[4] D. W. Snoke, Y. S. Raptis, and K. Syassen, Phys. Rev. B **45**, 14419 (1992).
[5] M. Núñez-Regueiro, L. Marques, J.-L. Hodeau, O. Bèthoux, and M. Perroux, Phys. Rev. Lett. **74**, 278 (1995).
[6] A. M. Rao, P. C. Eklund, J.-L. Hodeau, L. Marques, and M. Núñez-Regueiro, Phys. Rev. B **55**, 4766 (1997).
[7] L. Marques, M. Mezouar, J.-L. Hodeau, M. Núñez-Regueiro, N. R. Serebryanaya, V. A. Ivdenko, V. D. Blank, and G. A. Dubitsky, Science **283**, 1720 (1999).
[8] B. Sundqvist, Adv. Phys. **48**, 1 (1999).
[9] K. P. Meletov, J. Arvanitidis, E. Tsilika, S. Assimopoulos, G. A. Kourouklis, S. Ves, A. Soldatov, and K. Prassides, Phys. Rev. B **63**, 054106 (2001).
[10] R. Moret, Acta Crystallogr., Sect. A: Found. Crystallogr. **A61**, 62 (2005).
[11] K. P. Meletov, V. A. Davydov, A. V. Rakhmanina, V. Agafonov, and G. A. Kourouklis, Chem. Phys. Lett. **416**, 220 (2005).
[12] A. San Miguel, Chem. Soc. Rev. **35**, 876 (2006).
[13] S. Yamanaka, A. Kubo, K. Inumaru, K. Komaguchi, N. S. Kini, T. Inoue, and T. Irifune, Phys. Rev. Lett. **96**, 076602 (2006).
[14] R. Poloni, M. V. Fernandez-Serra, S. Le Floch, S. De Panfilis, P. Toulemonde, D. Machon, W. Crichton, S. Pascarelli, and A. San-Miguel, Phys. Rev. B **77**, 035429 (2008).
[15] O. Zhou, J. E. Fischer, N. Coustel, S. Kycia, Q. Zhu, A. R. McGhie, W. J. Romanow, J. P. McCauley, A. B. Smith, and D. E. Cox, Nature (London) **351**, 462 (1992).
[16] P. Zhou, K.-A. Wang, Y. Wang, P. C. Eklund, M. S. Dresselhaus, G. Dresselhaus, and R. A. Jishi, Phys. Rev. B **46**, 2595 (1992).
[17] G. Dresselhaus, M. S. Dresselhaus, and P. C. Eklund, Phys. Rev. B **45**, 6923 (1992).
[18] G. Meijer and D. S. Bethune, Chem. Phys. Lett. **175**, 1 (1990).
[19] K.-A. Wang, Y. Wang, P. Zhou, J. M. Holden, S. L. Ren, G. T. Hager, H. F. Ni, P. C. Eklund, G. Dresselhaus, and M. S. Dresselhaus, Phys. Rev. B **45**, 1955 (1992).

[20] Y. S. Raptis, D. W. Snoke, K. Syassen, S. Roth, P. Bernier, and A. Zahab, High Press. Res. **9**, 41 (1992).
[21] R. E. Stanton and M. D. Newton, J. Phys. Chem. **92**, 2141 (1998).
[22] R. A. Jishi and M. S. Dresselhaus, Phys. Rev. B **45**, 6914 (1992).
[23] S. Fujiki *et al.*, Phys. Rev. B **62**, 5366 (2000).
[24] R. C. Haddon *et al.*, Nature (London) **350**, 320 (1991).
[25] G. Lucazeau, J. Raman Spectrosc. **34**, 478 (2003).
[26] J. M. Soler, E. Artacho, J. D. Gale, A. García, J. Junquera, P. Ordejón, and D. S. Sanchez-Portal, J. Phys.: Condens. Matter **14**, 2745 (2002).
[27] J. Junquera, O. Paz, D. Sánchez-Portal, and E. Artacho, Phys. Rev. B **64**, 235111 (2001).
[28] E. Anglada, J. M. Soler, J. Junquera, and E. Artacho, Phys. Rev. B **66**, 205101 (2002).
[29] J. P. Perdew and A. Zunger, Phys. Rev. B **23**, 5048 (1981).
[30] S. Guha, J. Menéndez, J. B. Page, and G. B. Adams, Phys. Rev. B **53**, 13106 (1996).
[31] It should be noted here that 2D polymerized forms of C_{60}, in which the molecular character of C_{60} has been already partially lost, can be stabilized up to 30 GPa [K. P. Meletov, J. Arvanitidis, G. A. Kourouklis, K. Prassides, and Y. Iwasa, Chem. Phys. Lett. **357**, 307 (2002)].